Springer Series in Materials Science 180

M. S. Ramachandra Rao
Tatsuo Okada *Editors*

ZnO Nanocrystals and Allied Materials

Springer Series in Materials Science

Volume 180

Series Editors

Robert Hull, Charlottesville, VA, USA
Chennupati Jagadish, Canberra, ACT, Australia
Richard M. Osgood, New York, NY, USA
Jürgen Parisi, Oldenburg, Germany
Zhiming M. Wang, Chengdu, P.R. China

For further volumes:
http://www.springer.com/series/856

The Springer Series in Materials Science covers the complete spectrum of materials physics, including fundamental principles, physical properties, materials theory and design. Recognizing the increasing importance of materials science in future device technologies, the book titles in this series reflect the state-of-the-art in understanding and controlling the structure and properties of all important classes of materials.

M. S. Ramachandra Rao
Tatsuo Okada
Editors

ZnO Nanocrystals and Allied Materials

Editors
M. S. Ramachandra Rao
Department of Physics
Indian Institute of Technology Madras
Chennai
Tamil Nadu
India

Tatsuo Okada
Department of Electrical Engineering
Kyushu University
Fukuoka
Japan

ISSN 0933-033X ISSN 2196-2812 (electronic)
ISBN 978-81-322-1159-4 ISBN 978-81-322-1160-0 (eBook)
DOI 10.1007/978-81-322-1160-0
Springer New Delhi Heidelberg New York Dordrecht London

Library of Congress Control Number: 2013945152

© Springer India 2014
This work is subject to copyright. All rights are reserved by the Publisher, whether the whole or part of the material is concerned, specifically the rights of translation, reprinting, reuse of illustrations, recitation, broadcasting, reproduction on microfilms or in any other physical way, and transmission or information storage and retrieval, electronic adaptation, computer software, or by similar or dissimilar methodology now known or hereafter developed. Exempted from this legal reservation are brief excerpts in connection with reviews or scholarly analysis or material supplied specifically for the purpose of being entered and executed on a computer system, for exclusive use by the purchaser of the work. Duplication of this publication or parts thereof is permitted only under the provisions of the Copyright Law of the Publisher's location, in its current version, and permission for use must always be obtained from Springer. Permissions for use may be obtained through RightsLink at the Copyright Clearance Center. Violations are liable to prosecution under the respective Copyright Law.
The use of general descriptive names, registered names, trademarks, service marks, etc. in this publication does not imply, even in the absence of a specific statement, that such names are exempt from the relevant protective laws and regulations and therefore free for general use.
While the advice and information in this book are believed to be true and accurate at the date of publication, neither the authors nor the editors nor the publisher can accept any legal responsibility for any errors or omissions that may be made. The publisher makes no warranty, express or implied, with respect to the material contained herein.

Printed on acid-free paper

Springer is part of Springer Science+Business Media (www.springer.com)

Foreword

New opportunities are opening up for innovative materials research across physics, electrical sciences, chemistry, surface science, and nanotechnology. Keeping in line with this, the Department of Physics at IIT Madras organized a two-day workshop on ZnO nanocrystals and allied materials. This two-day conference was conducted by Indian collaborators from IIT Madras and Japanese collaborators from Kyushu University, Japan. Researchers from the academic world of India and Japan presented their recent results on the development of nanostructured ZnO and allied materials and their applications in key areas of Applied Physics and Electrical Engineering. The work presented by all the experts during the workshop has been compiled into this book form with carefully written contributory articles. This book thus presents complete articles summarizing 17 invited talks and contributions. It is well complemented by research work from various scientists well known in the field of ZnO and Allied Materials.

Progress in the nano-research based on ZnO, during the last decade, has been very fast. Various research programs have been renewed and revisited and efforts are on to remove the deadlocks with the help of accurate research on ZnO nanostructures and applied materials for routine use in industry worldwide. It was therefore considered timely to organize an Indo–Japan workshop. It takes a good collaborative effort to understand and explore the varied physical properties and to envisage device applications of ZnO in thin films, heterostructures, and nanostructures. ZnO has been the central theme of research in the past decade due to its potential as UV/blue light emitting diode material that can replace GaN if only the *p*-type doping problem is resolved. In nanostructured form, it offers ample opportunities to realize tunable optical and optoelectronic properties and it was also termed as a potential material to realize room temperature ferromagnetism. ZnO can be easily deposited in high quality thin film form by sputtering, CVD, and laser ablation methods at low temperatures. It can be easily fabricated into devices and its lattice is amenable to 3d and 4f element doping. ZnO is biocompatible and exhibits many interesting applications in textile and biomedical industries. Doping in ZnO can bring about changes in optical emissivity and by virtue of controlling the oxygen vacancies, ZnO lattice can be used for light emission in a wide spectral range. Al doped ZnO competes well with ITO for easy fabrication of conducting

back electrodes for solar cells. ZnO quantum dots open new technological avenues for the fabrication of photonic crystal lattices. ZnO heterostructures can play a key role in band gap engineering. Alloys of MgZnO are useful in tuneable band gap systems and many of its allied material systems can be used in gas sensing applications.

The fundamental challenge, however, remains the same: more stable *p*-type ZnO and its application to larger systems, and access to new materials properties. Responding to these challenges will require substantial effort at various levels.

Being the workshop organizers and editors of this book, we would like to thank all the contributors (especially those who accepted the burden of writing full chapter articles) and the members of the Advisory Board for helping to organize such an effective program. We are sure that this book with an assortment of articles will be quite useful for researchers in this area.

M. S. Ramachandra Rao
Tatsuo Okada

Preface

Functional nanostructures are attracting much interest for use in sensing, energy harvesting, and flexible electronics. ZnO is a versatile material system that offers potential applications in high power and high temperature electronics, UV/Visible light emitting diodes for domestic lighting, and in colour displays. Due to its radiation hardness property, it also finds application in radiation hard transistors for high temperature sensors and spaceflight instrumentation. There have been many recent advances in this field, concerning nanostructure synthesis. ZnO has also been reported as an active channel material for thin-film transistors because of its high electron mobility even for room temperature deposition in ZnO (as the semiconducting active layer)-based field effect transistors. ZnO has also attracted significant attention as a new candidate for transparent electrodes due to its good conductivity, high optical transparency, and surface smoothness.

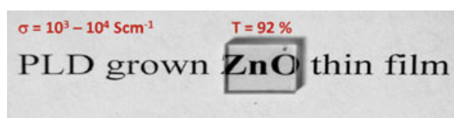

This book brings together articles contributed by experts working on various aspects of ZnO and allied materials detailing all the important recent advances. The topics begin with a brief review of ZnO followed by an important article on nano-Soldering of ZnO nanowires and GaN thin films for the fabrication of hetero *p-n* junction using laser. The book also presents works on photoluminescence processes of ZnO thin films and quantum structures, Li–Ni co-doped ZnO films grown by pulsed laser deposition for realizing stable *p*-type conducting material, lasing characteristics of an optically pumped single ZnO nanocrystal, and nanomachining for controlling oscillation wavelength, deposition of Al-doped ZnO films by ICP-assisted sputtering. Advances in nanoparticle-assisted pulsed laser deposition, synthesis of silicon carbide (SiC) thin films using pulsed laser deposition, ZnO-based phosphors, related bio-material applications, experimental

and theoretical investigations of dopants, and defects in ZnO nanoparticles have also been discussed. The purpose of the book is to present a summary of the current state-of-the-art research aspects that can pave the way for new areas for future research.

M. S. Ramachandra Rao
Tatsuo Okada

Acknowledgments

Prof. M. S. R. Rao would like to thank the Department of Science and Technology (DST) funding that facilitated the establishment of Nano Functional Materials Technology Centre (NFMTC) at IIT Madras.

Prof. Okada would like to thank the financial support under the program of Special Coordination Funds for Promoting Science and Technology from Japan Science and Technology Agency (JST).

Our special thanks to Dr. Shubra Singh for careful editing and proof reading of the manuscripts.

Contents

1 Zinc Oxide: The Versatile Material with an Assortment of Physical Properties 1
E. Senthil Kumar, Shubra Singh and M. S. Ramachandra Rao

2 Laser Nano-Soldering of ZnO Nanowires and GaN Thin Film for Fabrication of Hetero *p-n* Junction 39
Tetsuya Shimogaki, Yuki Ishida, Kota Okazaki, Mitsuhiro Higashihata, Daisuke Nakamura and Tatsuo Okada

3 Photoluminescence Processes in ZnO Thin Films and Quantum Structures 49
L. M. Kukreja and P. Misra

4 Effect of Oxygen Pressure on Photoluminescence Spectra and Hall Coefficients of Li–Ni Co-Doped ZnO Films Grown by a Pulsed Laser Deposition 91
K. Sakai, K. Ishikura, D. Ohori, D. Nakamura, A. Fukuyama, T. Okada, M. S. Ramachandra Rao and T. Ikari

5 Lasing Characteristics of an Optically-Pumped Single ZnO Nanocrystal and Nanomachining for Controlling Oscillation Wavelength 101
K. Okazaki, T. Shimogaki, I. A. Palani, M. Higashihata, D. Nakamura and T. Okada

6 Deposition of Aluminum-Doped ZnO Films by ICP-Assisted Sputtering 125
Yoshinobu Matsuda, Akinori Hirashima, Kenji Mine, Takuhiro Hashimoto, Daichi Matsuoka, Masanori Shinohara and Tatsuo Okada

7 Control of ZnO Nano-Crystals Synthesized by Nanoparticle-Assisted Pulsed Laser Deposition Using Buffer Layer and Laser Irradiation 149
Daisuke Nakamura, Tetsuya Shimogaki, Kota Okazaki, I. A. Palani, Mitsuhiro Higashihata and Tatsuo Okada

8 Influence of Sb as a Catalyst in Synthesize of Sb Doped ZnO Nanostructures Using Nanoparticle Assisted Pulsed Laser Deposition for UV LED Applications 175
I. A. Palani, D. Nakamura, K. Okazaki, M. Highasiata and T. Okada

9 Time and Spatially Resolved Luminescence Spectroscopy of ZnO Nanostructures 195
Hideaki Murotani, Yoichi Yamada, Daisuke Nakamura and Tatsuo Okada

10 Synthesis of Polycrystalline Silicon Carbide (SiC) Thin Films Using Pulsed Laser Deposition 217
B. Venkataramesh and Nilesh J. Vasa

11 Preparation and Characterization of ZnO Nanorods, Nanowalls, and Nanochains 233
T. Premkumar, Y. F. Lu and K. Baskar

12 Synthesis and Characterization of ZnO-Based Phosphors and Related Phosphor Composites in Bulk, Thin Film and Nano Form 247
P. Thiyagarajan, M. Kottaisamy and M. S. Ramachandra Rao

13 Zinc Oxide Nanomaterials as Amylase Inhibitors and for Water Pollution Control 269
Rohini Kitture, Sandip Dhobale and S. N. Kale

14 Zinc Oxide: From Optoelectronics to Biomaterial—A Short Review 289
R. Suryanarayanan

15 On the Optical and Magnetic Properties of Doped-ZnO 309
J. Kumar, S. Ramasubramanian, R. Thangavel and M. Rajagopalan

16 Low-Temperature Photoluminescence of Sb-doped ZnO Nanowires Synthesized on Sb-coated Si Substrate by Chemical Vapor Deposition Method 331
K. Sakai, K. Ishikura, A. Fukuyama, I. A. Palani, M. S. Ramachandra Rao, T. Okada and T. Ikari

17 Experimental and Theoretical Investigations of Dopant, Defect, and Morphology Control on the Magnetic and Optical Properties of Transition Metal Doped ZnO Nanoparticles 341
O. D. Jayakumar, C. Persson, A. K. Tyagi and C. Sudakar

Editors Biography 371

Author Index 373

Chapter 1
Zinc Oxide: The Versatile Material with an Assortment of Physical Properties

E. Senthil Kumar, Shubra Singh and M. S. Ramachandra Rao

Abstract Zinc oxide has the potential to replace GaN as the next-generation white light emitting diode material. This wide bandgap semiconductor with an excitonic binding energy of ~ 60 meV has been researched extensively in the last decade due to its immense potentiality for blue/UV light emitting devices. ZnO lattice is amenable to doping with transition metal ions (TM) and 4*f*-elements. Such a doping activity in ZnO has been mainly aimed at the realization of *n* and *p*-type conductivity and room temperature diluted magnetic semiconducting behavior. Several doping studies have been attempted in order to get an insight into the changes in physical properties with the emphasis on fabricating of all ZnO *p*–*n* junctions for white light/UV emission. The challenge is to obtain highly stable *p*-ZnO with doping. Our group has been working on doping studies in ZnO. Ni doping shows a dramatic decrease in resistivity in polycrystalline ZnO. Stable and low resistive *p*-type conduction in ZnO was not possible with monovalent ion (Li, Ag etc.) doping. Recent work indicated the possibility of inducing shallow holes into ZnO lattice using co-doping route. We used Li and Ni co-doping to realize a low resistive, *p*-type and magnetic ZnO. Aligned 1-dimensional ZnO nanowires can also be obtained using PLD and other methods. Our research group at IIT Madras has been working closely with Kyushu University and other partner universities in Japan to make research in ZnO a worthwhile attempt aimed at device applications. We will present, in this chapter, overall physical properties of ZnO with our important results related to the doping aspects in ZnO.

E. Senthil Kumar · M. S. Ramachandra Rao (✉)
Department of Physics, Nano Functional Materials Technology Centre,
and Materials Science Research Centre, Indian Institute of Technology (IIT) Madras,
Chennai 600036, India
e-mail: msrrao@iitm.ac.in
URL: www.physics.iitm.ac.in/~msrrao

S. Singh
Crystal Growth Centre, Anna University, Chennai 600025, India

M. S. R. Rao and T. Okada (eds.), *ZnO Nanocrystals and Allied Materials*,
Springer Series in Materials Science 180, DOI: 10.1007/978-81-322-1160-0_1,
© Springer India 2014

1.1 Introduction

In the past two decades, optoelectronics research was mainly focused on the crystal growth and conductivity control of semiconductors such as SiC, II–VI chalcogenides, III–V compound semiconductors, and II–VI metal oxides [1–3]. Despite the successful fabrication of SiC-based blue light-emitting diodes (LEDs) and considerable research efforts devoted to the fabrication of *p*-type ZnSe and II–VI blue-green lasers, these two semiconductors were rapidly outshined by the superior electronic properties and light emission efficiency of nitride-based thin-film devices (Morkoc et al. 1994). Furthermore, the external quantum efficiency of nitride-based LEDs in the blue region was found to surpass that of SiC LEDs (41 % for nonpolar InGaN/GaN LEDs vs 0.3 % for SiC LEDs) [4]. The success of III–V nitrides was due to the achievement of stable *p*-type behavior and low resistivity in GaN thin films doped with Mg [5]. These breakthroughs led to the possible fabrication of small sized and high-brightness blue light emitting devices and laser diodes [6]. These devices find applications in high-storage capacity optical recording media (e.g., Blu-ray disks) and optical communication. There is also a large potential in lighting and illumination such as traffic signals, automobile interior panel lighting, high-resolution printers, video game consoles, ophtalmics, and biophotonics [7].

In parallel with nitrides, oxide semiconductors continue to receive considerable attention due to their low cost of fabrication, chemical robustness, and high thermal conductance [8]. Transparent conducting oxide thin films such as Sn-doped In_2O_3 (ITO), F-doped SnO_2, and Al-doped ZnO are usually fabricated on transparent substrates such as glass or sapphire [9, 10]. These semiconductors always exhibit *n*-type conduction with a resistivity of 10^{-4}–10^{-5} Ω cm and are widely used as transparent electrodes in thin film transistors, organic light emitting diodes, and solar cells. The lack of transparent *p*-type oxide material has always been a major obstacle to the fabrication of oxide-based *p–n* homo and hetero-junction devices.

Zinc oxide (ZnO) is a II–VI transparent conducting oxide touted as a material of choice for short wavelength optoelectronics. Similar to GaN, ZnO has a direct band gap of 3.37 eV at 300 K that can be engineered via dilute alloying with BeO, MgO, and CdO [11–13], while retaining its wurtzite structure. As shown in Fig. 1.1, the more tightly bound exciton in ZnO (60 meV) compared with other compound semiconductors (20 meV for GaN) opens the possibility for ZnO-based optoelectronic devices to operate well above 300 K. Lasing in optically pumped ZnO has already been demonstrated at 300 K in high-quality epilayers, polycrystalline films (random lasers), quantum well superlattices, and nanowire arrays [14–16]. Furthermore ZnO, which shows electron and proton radiation hardness capabilities, can be of potential use in high-irradiation conditions such as space-based environments.

ZnO and its ternary alloys have the potential to compete with III–V nitrides for optoelectronic applications. However, fabrication of the ZnO-based optoelectronic

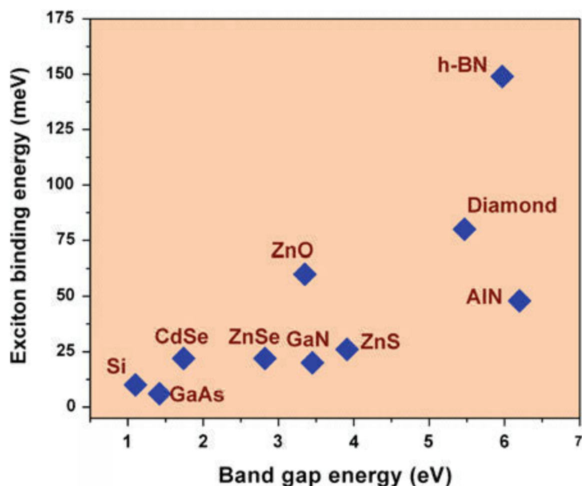

Fig. 1.1 The exciton binding energy as a function of the band gap energy for compound semiconductors

devices is still a problem to deal with due to the difficulty in obtaining *p*-type ZnO. The quest for stable, *p*-type ZnO is a challenging one because the electrical and optical properties of ZnO are very sensitive to minute concentrations of dopants, impurities, and to microscopic perturbations of the lattice [17]. It will be explained in the subsequent sections that the reasons for the difficulties to achieve *p*-type ZnO come from its asymmetric defect chemistry, ionicity, and the complex roles of impurities and crystal defects.

The observation of ferromagnetism in (Ga, Mn) As has inspired a great deal of research interest in the field of spintronics [18]. The main challenge for practical application of the diluted magnetic semiconductor (DMS) materials is the attainment of Curie temperature (T_C) at or preferably above room temperature. Transition metal (TM) ion-doped ZnO became the most extensively studied topical material, since the prediction by Dietl et al. [19], as a promising candidate to realize Curie temperature above room temperature. The particular predictions are on the assumption that hole mediated exchange interaction is responsible for magnetic ordering. The additional advantages of ZnO-based DMSs are that they can be readily incorporated into the existing semiconductor heterostructure systems, in which a number of optical and electronic devices have been realized, thus allowing the exploration of the underlying physics and applications based on previously unavailable combinations of quantum structures and magnetism in semiconductors.

Low-dimensional self-assembled ZnO nanostructures have shown a great advantage in fabrication of devices in the nanometer regime. In particular, one-dimensional (1D) ZnO nanowires/rods have been used to fabricate the field emission devices, piezoelectric nanogenerators, photonic devices, and light emitting diodes [20]. When the sizes of the ZnO nanostructures are comparable with that of exciton Bohr radius, excellent quantum confinement effects have been seen in the optical and electrical properties of ZnO (Song et al. 2007).

Table 1.1 Comparison of physical properties of some key compound semiconductors

Material	Crystal structure	Lattice constants *a* and *c* (Å)	Band gap (eV)	Energy of fusion (K)	Exc. binding energy (meV)	Dielectric constant ε (0) and ε (∞)
ZnO	Wurtzite	3.25	3.37	2,248	60	8.75
		5.21				3.75
ZnS	Wurtzite	3.82	3.8	2,103	30	9.6
		6.26				5.7
ZnSe	Zinc blende	5.66	2.7	1,793	20	9.1
						6.3
GaAs	Zinc blende	5.65	1.43		4.2	12.9
						10.9
GaN	Wurtzite	3.19	3.39	1,973	21	8.9
		5.19				5.35
SiC	Wurtzite	3.18	2.86	>2,100	–	9.66
		15.12				6.52

Hence, in this article we have made an effort to explore the electrical, magnetic, and optical properties of doped and undoped ZnO thin films and nanostructures. Table 1.1 shows the summary of the physical properties of some key compound semiconductors used for the optoelectronic applications. It is evident that the ZnO is the only oxide counterpart to GaN in terms of band gap and exciton binding energy. In addition, ZnO is one of the promising transparent conducting oxide used for as transparent electrode in solar cells.

1.2 Physical Properties of ZnO

In this section, crystal structure, electronic band structure, doping studies, transport properties, magnetic properties, and optical properties of the ZnO will be discussed in detail.

1.2.1 Crystal Structure

ZnO is a II–VI compound semiconductor, which crystallizes into three different structures viz., wurtzite (B4), zinc blende (B3), and rocksalt (B1) under different growth conditions. Where B1, B3, and B4 denote *strukturbericht* designations for the three phases [21]. Among these structures, the wurtzite structure is thermodynamically most stable phase under ambient conditions. The zincblende structure can be stabilized by growing on cubic substrates like MgO and Pt/SiO_2/Si [11]. However, the rocksalt (NaCl) structure can be realized only by applying very high

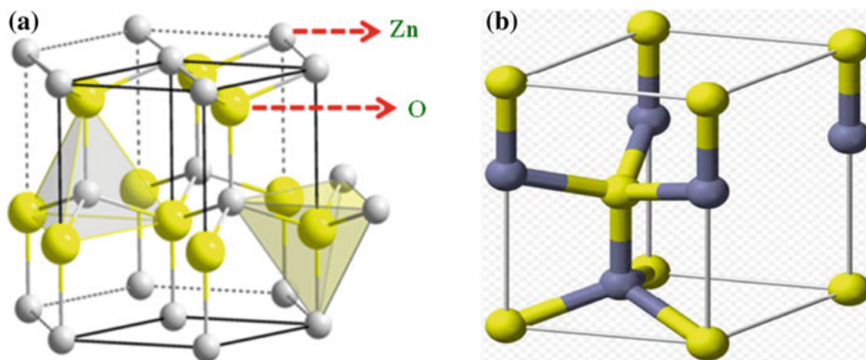

Fig. 1.2 **a** Wurtzite crystal structure of ZnO showing the tetrahedral coordination of the Zn and O atoms. **b** Unit cell of wurtzite structure (figure: courtesy http://www.en.wikipedia.org/wiki/Zinc_oxide)

pressures [22]. When compared with zincblende and rocksalt structures, wurtzite ZnO has shown intriguing optical, electrical, and optoelectronic properties in thin film and nanostructured form. Hence, a lot of research work has been mainly focused on the study of doped and undoped wurtzite ZnO thin films and nanostructures.

The wurtzite ZnO belongs to the space group of C_{6v}^{4} in the Schoenflies notation and $P6_3mc$ in Hermann–Mauguin notation [23]. Figure 1.2 shows the crystal structure and unit cell of the wurtzite ZnO. The structure is composed of two interpenetrating hexagonal close packed (hcp) sublattices, each of which consists of one type of atom displaced with respect to each other along the three fold c-axis by the amount $u = 3/8 = 0.375$, where the parameter u is defined as the anion–cation bond length parallel to the c-axis. The measured lattice parameters of the hexagonal wurtzite ZnO are $a = 3.249$ Å and $c = 5.206$ Å. In the wurtzite ZnO, each sublattice consists of four atoms per unit cell and each atom of one kind is surrounded by four atoms of the other kind. In other words, both Zn and O atoms are tetrahedrally coordinated to each other. This tetrahedral coordination gives rise to polar symmetry along the c-axis.

The polar nature of the ZnO is responsible for many interesting properties viz., piezoelectricity, spontaneous polarization, crystal growth, etching, and defect generation. In ZnO, both Zn terminated (0001) and O terminated $(000\bar{1})$ faces are polar in nature. The other important faces in the wurtzite ZnO structure are nonpolar $(11\bar{2}0)$ and $(10\bar{1}0)$. Figure 1.3 gives the important planes and orientations that are commonly seen in wurtzite structure.

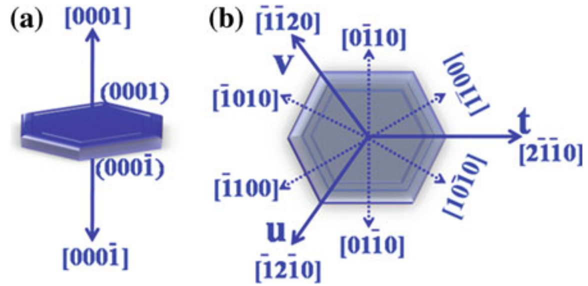

Fig. 1.3 **a**, **b** Various polar and nonpolar planes in ZnO hexagonal wurtzite structure

1.2.2 Electronic Band Structure

Numerous theoretical calculations have been employed to calculate the band structure of ZnO by a number of groups [24]. Figure 1.4 shows the calculated band structure of wurtzite crystal of ZnO. Location of the Zn 3*d* levels was unambiguously determined using the local density approximation (LDA) and incorporating atomic self-interaction corrected pseudo-potentials (SIC-PP). In ZnO, both the valence band maxima and the conduction band minima occur at the Γ point $k = 0$ indicating that ZnO is a direct band gap semiconductor. The bottom 10 bands, occurring around −9 eV (not shown in figure), correspond to Zn 3*d* levels [23]. The next six bands, from −5 to 0 eV, correspond to O 2*p* levels. The first two conduction band states are strongly Zn localized and correspond to empty Zn 3*s* states. The O 2*s* bands, associated with core-like energy states, occur around −20 eV. Using the above calculation, the band gap was determined as 3.77 eV. In addition to theoretical calculations, the electronic band structure was experimentally carried out [25], at the surface of wurtzite ZnO, using the data obtained from electron energy loss spectroscopy (EELS) and ultraviolet photoelectron spectroscopy (UPS). It was observed that the Zn face possesses more covalent character, arising from the Zn 4*s* – O 2*p* states, while the O face is more ionic.

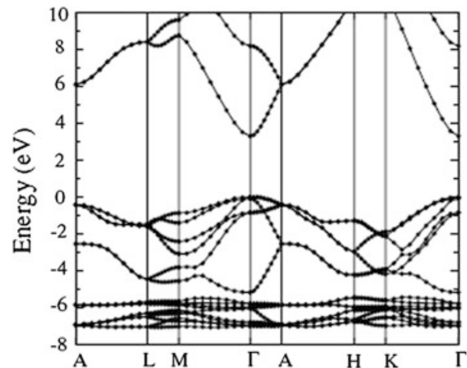

Fig. 1.4 Calculated band structure of the wurtzite ZnO using HSE hybrid functional method. Reprinted after permission from IOP publishing group (*Rep. Prog. Phys.* 72, 126501 (2009))

1.3 Doping Studies in ZnO

The physical properties of ZnO are strongly affected by the dopant impurities and defects. ZnO exhibits intriguing electrical, optical, and magnetic properties when doped with TM ions and other elements [23]. These properties can be tuned by carefully controlling the defects and concentration of dopant impurities in the system. The future optoelectronic applications of ZnO will depend on the ability to dope it into *n*-type and *p*-type material. Band gap of the ZnO can be engineered by doping with Cd and Mg.

1.3.1 Defects in ZnO

The electrical and optical properties of ZnO are still not well understood, which implies that the role of various extrinsic as well as intrinsic defects have not been clearly understood yet. In this section, some of the experimental as well as theoretical approaches to illustrate the presence of defects will be explained. An old age saying in materials science goes as, "materials are like people; it is the defects that make them interesting". Defects play an important role in determining the electronic and optoelectronic properties of semiconducting materials. However, we need to identify and quantify these defects in order to understand the microscopic processes involved. Different types of defects come into effect due to different growth conditions, doping, and growth techniques. Occurrence of electronic defects, involved in optical recombination processes, depends on structure, particle size, composition as well as crystallinity of the sample. A fundamental understanding of the physics of various defects can help in improving emission properties of ZnO as well as in achieving *p*-type conduction in this compound. Appreciable amount of work have been reported on the intrinsic as well as extrinsic defect species present in this compound [26–31]. However, most of these papers present controversial results. Sun et al. studied the intrinsic defects in ZnO by using full potential linear muffin-tin orbital method, and concluded that zinc interstitial is the dominant donor owing to its shallower defect level [32–34]. Kohan and Van de Walle [33, 34] seperately studied different possible native point defects in ZnO by the plane-wave pseudopotential method in the LDA. Kohan et al. [33] used the first-principles pseudopotential method to determine the electronic structure, atomic geometry, and formation energy of native point defects in ZnO and showed that both the Zn and O vacancies are the relevant defects in ZnO. Zhang et al. [35] also calculated the formation energies of native defects in ZnO by the plane-wave pseudopotential method in the LDA. Oxygen and zinc vacancies were found to have the lowest formation energies in their calculations, but the formation energies of most defects have a considerable difference from Kohan's results. Oba et al. [36] calculated the electronic structure of native defects in ZnO by the plane-wave pseudo potential method in the generalized gradient

approximation (GGA), and showed that oxygen vacancies and zinc vacancies act as dominant donor and acceptor defects with deep levels, in agreement with Kohan's and Zhang's LDA studies and that zinc interstitials and zinc antisites are shallow donors. Other theoretical analyses have also shown that Zn interstitial is actually a shallow donor [35, 36] which was further supported by electron irradiation measurements. Kohan et al. [33] also show that oxygen vacancies have lower formation energy than the zinc interstitial defects and hence should be more abundant. Mahan's [26] interpretation of Hagemark's [29] experimental measurements agrees well with the results of Kohan et al. [33]. When there is excess Zn, the native donors are the oxygen vacancies and when there is Zn depletion, Zn vacancies are present [the formation energy of a Zn interstitial is at least 1.2 eV higher than that of an oxygen vacancy]. The formation energy of Zn and oxygen antisites has been found to be higher than that found in the case of Zn and O vacancy defects and hence the antisites are less likely to form [33]. For ZnO exposed to hydrogen during growth, it (hydrogen) was considered as the main donor (as it can ionize easily with low formation energy) [37]. The differences in concentrations of relevant point defects are determined by differences in formation energies of intrinsic point defects in wurtzite ZnO [38]. Electronic structure, formation energies, transition levels, and concentration of intrinsic defects in wurtzite ZnO were investigated by the projector augmented wave (PAW) method and it was found that oxygen and zinc vacancies are the dominant intrinsic donor and acceptor defects in ZnO [38]. Presence of defects can also affect the carrier concentration in ZnO [38]. In a solid, the defect is a function of the chemical potential of the species involved. At thermodynamic equilibrium, the concentration of defects in a crystal is given by the expression:

$$C_{\mathrm{d}} = N_{\mathrm{sites}} N_{\mathrm{config}} - \left(E_f / k_{\mathrm{B}} T\right) \tag{1.1}$$

Here, E_{f} is the formation energy of the defect. N_{sites} is the number of sites in the lattice (per unit volume) where the defect can be produced; N_{config} is the number of equivalent configurations. For a perfect ZnO crystal, the carrier concentration is

$$n_{\mathrm{e}} = n_{\mathrm{h}} = (N_{\mathrm{C}} N_{\mathrm{V}})^{1/2} \exp\left(-E_{\mathrm{g}} / 2k_{\mathrm{B}} T\right) \tag{1.2}$$

where n_{e} and n_{h} are the concentration of free electrons and holes respectively, k_{B} is the Boltzmann constant and T is the temperature. N_{C} and N_{V} are the effective density of states of the conduction and valence band respectively. For a ZnO crystal with defects, the carrier concentration depends upon the Fermi level in the following way:

$$n_e = N_C \exp\left[-\left(E_g - E_F\right) / k_B T\right], \quad n_h = N_V \exp(-E_F / k_B T) \tag{1.3}$$

Here, the Fermi level E_{F} is determined by the overall charge neutrality [39], i.e.

$$\sum q(i) N_{\mathrm{s}}(i) \exp\left[-E_{\mathrm{f}}^{(q)}(i) \Big/ k_{\mathrm{B}} T\right] = N_{\mathrm{C}} \exp\left[-\left(E_{\mathrm{g}} - E_{\mathrm{F}}\right) / k_{\mathrm{B}} T\right] - N_{\mathrm{V}} \exp(-E_{\mathrm{F}} / k_{\mathrm{B}} T) \tag{1.4}$$

Here, $E_f^{(q)}$ (i) is the formation energy of defect i at charge state q and $N_s(i)$ is the number of sites where defect i can be formed per unit volume. In the oxygen deficient condition, the most abundant native defect in ZnO is the oxygen vacancy, which acts as the dominant intrinsic donor. In the oxygen rich condition, the zinc vacancy is the most abundant native defect and serves as the dominant intrinsic acceptor. Zinc interstitial was also found to act as a dominant intrinsic donor in some studies [29, 30]. However, calculations by Zhao et al. [38] indicate that the zinc interstitial is at least 1.0 eV higher in formation energy than the oxygen vacancy. They also found that the formation energy of the oxygen interstitial is about 1 eV higher than that of the zinc vacancy. Some of the authors pointed out Zn interstitials as the dominant defects in ZnO, on the basis of ionic diffusion or size considerations [29, 40, 41], whereas others indicated that it was oxygen vacancies, based on the calculation of reaction rates, diffusion experiments, or electrical conductivity and Hall effect measurements [26].

Bulk ZnO crystals, grown by the seeded vapor phase and melt technique, have been found to have low concentration of defects, dominant one being the Zn vacancies Tuomisto and Look (2007). Zn vacancies as well as high concentrations of O vacancies have been observed in ZnO bulk crystals grown by conventional chemical vapor transport and hydrothermal methods [31].

The luminescence properties of ZnO have also been related to various crystalline lattice defects [42]. The internal absorption is not expected to affect the visible emission spectrum in wide bandgap semiconductors, hence the intensity of deep level emission should be roughly proportional to the density of defects present. Bond lengths associated with the host compounds are affected by the presence of defects (which can be explained in terms of size and charge effects). As for example Zn, vacancy defect implies the removal of a small positively charged Zn ion. Thus, we expect that other positively charged Zn ions will move closer to the vacant sites because of the availability of space and reduced electrostatic repulsion. Oxygen neighbors are no longer electrostatically attracted to the vacancy and consequently move farther away [33].

1.3.2 Electrical Properties of ZnO

Defect chemistry plays a very important role in controlling the electrical transport properties of ZnO [43]. ZnO belongs to a group of transparent conducting oxide (TCO) materials that show strong doping asymmetry (unipolarity) i.e., inability to dope both n and p-type carriers into the lattice.

Table 1.2 gives the summary of the electrical properties such as electron concentration and mobilities of the bulk ZnO and thin films grown by various techniques. Normally, these samples show n-type conductivity due to various defects present in the lattice.

Table 1.2 Summary of the electrical properties of the bulk ZnO and thin films grown by various techniques

Sample	Carrier concentration (cm^{-3})	Electron mobility ($cm^2 V^{-1} s^{-1}$)	Reference
Bulk ZnO grown by vapor-phase transport	6.0×10^{16}	205	Look et al. [46]
Bulk ZnO grown by pressurized melt method	5.05×10^{17}	131	Nause and Nemeth et al. [117]
Bulk ZnO grown by hydrothermal method	8×10^{13}	200	Maeda et al. [118]
PLD grown ZnO thin films on *c*-plane sapphire	2.0×10^{16}	155	Kaidashev et al. [119]
MBE grown ZnO thin films on *c*-plane sapphire	1.2×10^{17}	130	Kato et al. [44]
MBE grown ZnO thin films on *a*-plane sapphire	7.0×10^{16}	120	Iwata et al. [45]
PLD grown $Zn_{0.9}Mn_{0.1}O$/ZnO heterostructure on sapphire	8.8×10^{14}	130	Edahiro et al. [120]
MBE grown ZnO thin film on ZnO/MgO double buffer layers	1.2×10^{17}	145	Miyamoto et al. [121]
ZnO film grown on MgZnO-buffered ScAlMgO4 by PLD	1×10^{16}	440	Ohtomo and Tsukazaki [122]

1.3.2.1 *n*-Type Doping

Naturally, unintentionally doped ZnO shows *n*-type conduction with an electron concentration $\sim 10^{17}$–10^{21} cm^{-3} [44, 45]. It was believed that the *n*-type conduction originates due to native defects such as oxygen vacancies (O_v) and zinc interstitials (Zn_i). Look et al [46] suggested that zinc interstitials (Zn_i) are the dominant shallow donors, rather than O_v, with an ionization energy of about 30–50 meV. However, first-principle calculations show that both O_v and Zn_i have high formation energies in *n*-type ZnO, and therefore none of these native defects are shallow donors [33]. Van de Walle [37] has theoretically shown that H is likely to be the dominant background shallow donor in ZnO materials that are exposed to H during growth. Since the H mobility is large, it can easily diffuse into ZnO in any kind of growth technique. A recent theoretical calculation of Kim and Park [47] suggests that the columbic attraction between O_v and Zn_i acts as shallow donors in ZnO. Nevertheless, the origin of *n*-type conductivity in unintentionally doped ZnO is still a controversial and has not been completely understood.

Besides the native defects and H donors, the *n*-type doping of ZnO can be easily achieved by group-III elements and group-VII elements. Group-III elements such as Al, Ga and In can be easily substituted at Zn site with doping concentration $\sim 10^{20}$ cm^{-3} (Makino et al. 2004). Al-doped ZnO thin films grown by metal organic chemical vapor deposition (MOCVD) and pulsed laser deposition (PLD) methods have shown a low resistivity of 6.2×10^{-4} and 8.5×10^{-5} Ω cm

respectively [48, 49]. Ga-doped ZnO thin films grown by CVD method showed room temperature resistivity of $1.2 \times 10^{-4}\ \Omega$ cm [50]. These films are found to be transparent to visible light with transparency >90 %. Hence, Al or Ga-doped ZnO thin films can be an alternative for Indium Tin Oxide (ITO) for commercial applications in solar cells and flat panel displays due to their low cost, chemical and thermal stability, and nontoxicity.

1.3.2.2 *p*-Type Doping

Most of the wide bandgap semiconductors such as GaN, ZnO, ZnS, and ZnSe can be easily doped into *n*-type, while *p*-type doping is difficult [51]. ZnO has proven to exhibit strong unipolarity (*n*-type) i.e., doping asymmetry. The problem of *p*-type doping in ZnO can arise for several reasons such as (i) acceptor dopants may be compensated by the native donors (O_v and Zn_i) and background *H* impurities, (ii) low solubility of the dopant impurities, and (iii) high activation energy of acceptors (deep impurity level) [52]. The self compensation problem is the most challenging phenomenon in ZnO that leads to the instability of *p*-ZnO and reverting to *n*-type within a matter of days.

The possible *p*-type dopants in ZnO are group-IA and -IB elements (Li, Na, K, Ag, and Cu), group-V elements (N, P, Sb, and As), and Zn vacancies (Zn_v) [53–55]. However, many of these form deep acceptor levels and do not contribute significantly to the *p*-type conduction. It has been believed that the most promising dopants for *p*-type ZnO are the group-V elements, although theoretical studies suggest some difficulty in achieving shallow acceptor levels [56]. In order to understand the microscopic aspects of *p*-type doping in ZnO, numerous theoretical studies have been made using first-principle calculations [57]. It was shown that group-I elements may be better *p*-type dopants than group-V elements in terms of the shallowness of acceptor levels. However, in contrary, group-I elements tend to occupy interstitial sites rather than substitutional sites because of their small ionic radii [38]. Doping with K and Na increases the Zn–O bond length that leads to the formation of compensating donor defects. Similarly, P and As doping in ZnO increases the bond length and hence they form antisites, A_{Zn}, which are well-known donors in ZnO [57]. N substitution at the O site is believed to be the best *p*-type doping in ZnO [53, 58]. However, a few theoretical and experimental reports show that N can form a deep acceptor level in ZnO [56, 56]. Moreover, the stability of N in ZnO is found to be low [59].

Yamamoto and Yoshida [52] proposed a codoping method to solve the unipolarity in ZnO, based on ab-initio electronic band structure calculations. Codoping acceptors (N) with donor impurities (Ga, Al and In) in the 2:1 ratio in ZnO was suggested to stabilize the N in appropriate lattice site through acceptor–donor–acceptor (N–Ga–N) formation [60]. The enhancement of solubility limit was explained in terms of the formation of ionic pairs between donor and acceptor ions as a consequent reduction in Madelung energy. The calculated differences in Madelung energy (E_{Mad}) between (i) undoped and group-III doped, (ii) undoped

Table 1.3 Calculated differences in Madelung energy (E_{Mad}) between undoped and *n* or *p*-type doped ZnO

n-type doping		*p*-type doping		Codoping	
Element	E_{Mad}	Element	E_{Mad}	Element	E_{Mad}
Al	−6.44	N	+0.79	(Al, 2 N)	−3.95
Ga	−13.72	Li	+13.56	(Ga, 2 N)	−11.27
In	−9.73	As	+12.61	–	–

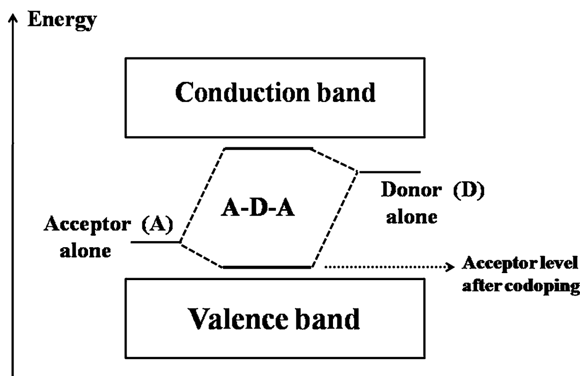

Fig. 1.5 Schematics depicting a change in acceptor and donor energy levels in the band gap due to the strong interaction between acceptors and reactive donors

and group-V doped, and (iii) undoped and Group-III and V codoped ZnO system are shown in Table 1.3. It is very clear from the table that the Madelung energy decreases with the group-III elements (Al, Ga, and In) for *n*-type doping, whereas it increases with group- I and V elements (Li, N and As) for *p*-type doping.

Yamamoto [60] have shown that the codoping method causes the formation of the complexes including acceptors and donors in the crystals, and contributes (i) to reduce the Madelung energies and enhance the incorporation of acceptors because the strong acceptor–donor attractive interaction overcomes the repulsive interactions between the acceptors and (ii) to lower the energy levels of the acceptors in the band gap due to the strong interaction between the acceptors and donors by forming an acceptor–donor–acceptor complex as shown in Fig. 1.5, and (iii) to increase the carrier mobility due to the short-range dipole-like scattering mechanism (long-range Coulomb scattering is dominated in the case of doping of acceptors alone). Thus, the *p*-type codoped semiconductors exhibit low resistivity with high carrier density and high mobility. Numerous experimental results have been successfully reported based on the codoping theory (Joseph et al. 1999) [9, 61].

Lee et al. [39] have suggested that codoping Li with H will be ideal for getting low resistive *p*-ZnO. However formation of the complexes, such as Li_{Zn}–Li_i, Li_{Zn}–H, and Li_{Zn}–AX, will limit the *p*-type doping concentration [62]. Zeng et al. [38] have reported a low resistivity of 16.4 Ω cm with a carrier mobility of 2.65 $cm^2\ V^{-1}\ s^{-1}$ by Li monodoping. The same group [63] has tried Li–N dual-acceptor doping in ZnO (ZnO: Li–N) and achieved a resistivity of 0.93 Ω cm and a Hall mobility of 0.75 $cm^2\ V^{-1}\ s^{-1}$ with an acceptor activation energy of 95 meV. Shubra et al. [64]

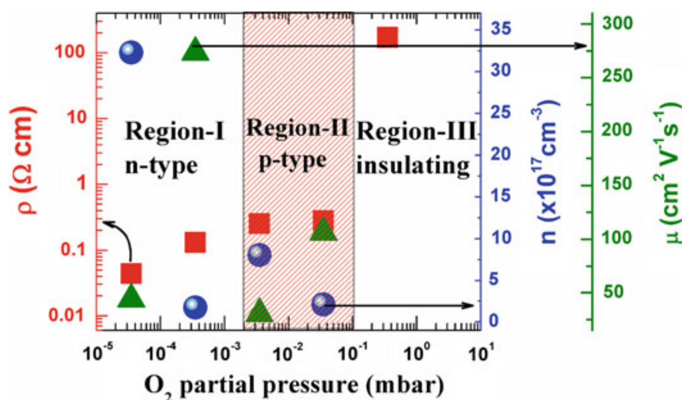

Fig. 1.6 Room temperature electrical transport properties of Li–Ni codoped ZnO thin films grown at various oxygen partial pressures. Reprinted after permission from American Institute of Physics (*Appl. Phys. Lett.* 96, 232504 (2010))

have reported a dramatic decrease in the bulk resistivity of Ni-doped ZnO. This was attributed to the impurity *d*-band splitting of Ni ion in the tetrahedral crystal field of ZnO. Recent experimental and theoretical reports [65, 66] show that incorporation of Li in TM ion-doped ZnO will stabilize the ferromagnetic ordering thereby increase the Curie temperature. However, what happens to the stability of *p*-type conduction when a TM ion is incorporated in Li-doped ZnO lattice, remains to be seen. This question has motivated us to examine the codoping of Li–Ni to achieve a stable and low resistive *p*-type ZnO. Hence Li–Ni codoped ZnO thin films were grown on sapphire substrates using PLD technique at a substrate temperature of 400 °C at with different oxygen partial pressures.

Room temperature electrical resistivity (ρ) of the Li–Ni codoped ZnO thin films is found to increase with the increase in oxygen growth pressure. The films grown at 10^{-5}, 10^{-4}, 10^{-3}, 10^{-2} and 10^{-1} mbar of oxygen partial pressure showed room temperature electrical resistivity of 0.044, 0.132, 0.254, 0.281, and 172 Ω cm, respectively. A dramatic jump in the electrical resistivity from 0.281 to 172 Ω cm is observed while increasing the oxygen partial pressure from 10^{-2} to 10^{-1} mbar. This is because at high O_2 partial pressures, a significant amount of Li occupies the interstitial sites (Li_i) and compensates the acceptors (Li_{Zn}), leading to an increase in the resistivity dramatically [62].

Room temperature Hall effect measurements on the Li–Ni codoped ZnO thin films grown at various oxygen partial pressures were carried out at a magnetic field of 8 T. Figure 1.6 shows the room temperature electrical transport properties of the Li–Ni codoped ZnO thin films as a function of oxygen growth pressure. We have observed three interesting conductivity regimes. The films grown at oxygen partial pressure in the range 10^{-5} and 10^{-4} mbar show *n*-type conductivity and exhibited electron concentrations of 3.2×10^{18} to 2.4×10^{17} cm^{-3}. The films grown at oxygen partial pressures $\geq 10^{-1}$ mbar exhibited insulating nature. Because of the high resistivity of these films, Hall effect measurements could not

be performed on these insulating films. However, we observed an interesting narrow window of growth pressure between 10^{-3} and 10^{-2} mbar, in which the films showed stable *p*-type conduction with a room temperature hole concentration of 8×10^{17} to 2.4×10^{17} cm^{-3} [67].

1.3.3 Magnetic Properties of ZnO

Diluted Magnetic Semiconductors (DMS) are semiconducting materials in which a fraction of the host cations can be substitutionally replaced by magnetic ions [68]. Much of the attention on DMS materials is due to its potential application in what is now called spintronic devices, in which both charge and spin can be simultaneously controlled [69, 70]. The III–V and II–VI semiconductors can be magnetically doped using the 3*d* TM ions and 4*f* rare-earth ions [71]. The discovery of hole mediated ferromagnetism in (Ga, Mn) As has paved the way for a wide range of possibilities for integrating magnetic and spin-based phenomena in microelectronics and optoelectronics [18]. However, the highest Curie temperature, T_C, reported in (Ga, Mn) As grown by molecular beam epitaxy (MBE), is $\sim$170 K [72]. In order to realize practical applications of spintronic devices, the DMS materials must exhibit ferromagnetism with a Curie temperature (T_C) above room temperature.

ZnO has attracted intense attention in the search for high T_C ferromagnetic DMS materials, since Dietl et al. [19] predicted that Mn-doped *p*-type ZnO-based DMSs could exhibit ferromagnetism above room temperature. This is due to the strong *p*–*d* hybridization between the *p*-states of the valence band and the Mn 3*d* levels. The values of T_C computed by assuming 5 % of Mn and $p = 3.5 \times 10^{20}$ cm^{-3}.

This prediction has stimulated considerable research in wide bandgap semiconductors, resulting in the observation of a spontaneous magnetic moment at room temperature in TM ion-doped nitrides and oxides. The wide bandgap semiconductors, which tend to have smaller lattice constants, exhibit strong *p*–*d* hybridization and small spin orbit interaction, and hence large Curie temperatures. In addition to the prediction of Dietl et al. [19], ferromagnetism in magnetic ion (V, Cr, Mn, Fe, Co, and Ni) doped ZnO has been theoretically investigated using ab-initio calculations based on the LDA by Sato et al. (2000, 2001). Their results suggest that ferromagnetic ordering can be possible even in *n*-type TM:ZnO thin films and bulk polycrystalline powders.

1.3.3.1 Origin of Ferromagnetism in TM Ion Doped ZnO

In a DMS material, presence of magnetic ions (TM ions) affects the free carrier behavior through the *sp*–*d* exchange interaction between the localized magnetic moments and the spins of the itinerant carriers [73]. Generally, 3*d* transition-metal ions substitute for the cations of the host semiconductors, i.e., Zn sites in ZnO.

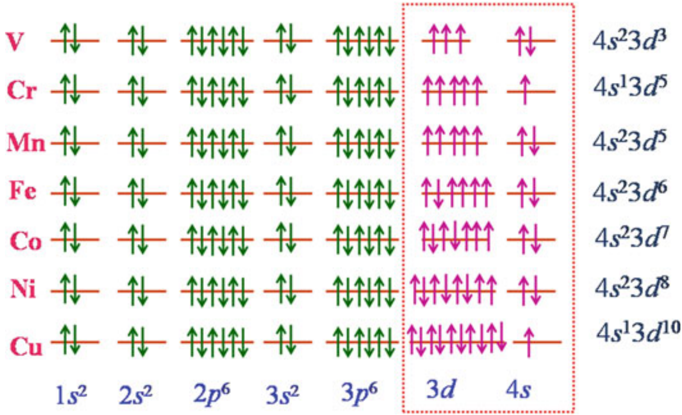

Fig. 1.7 Electronic configuration of the 3*d* states and 4*s* states of TM elements

In ZnO, the particular transition-metal element, for example, Mn, contributes its 4 s^2 electrons to the sp^3 bonding, and can therefore substitutionally replace the Zn in the tetrahedral bonding to form a TM^{2+} charge state. The 3*d* band of the Mn^{2+} ion is exactly half-filled with five electrons among the 10 available states. For other TM ions such as Fe, Co and Ni, one of the bands is usually partially filled (up or down), as shown in Fig. 1.7. The TM-*d* bands of the TM hybridize with the host valence bands (O-*p* bands in ZnO) to form the tetrahedral bonding. This hybridization gives rise to the exchange interaction between the localized 3*d* spins and the carriers in the host valence band. In this simple picture, the *s* band of the conduction band does not mix with the TM-*d* bands, but it is still influenced by the magnetic ion.

Few mechanisms proposed to understand the ferromagnetic properties of DMS materials are direct superexchange (antiferromagnetic), indirect superexchange (ferromagnetic), carrier mediated exchange (ferromagnetic) that include the double exchange mechanism and bound magnetic polarons (BMPs). In the Zener model, the direct interaction (superexchange) between the *d* shells of the adjacent Mn ions leads to antiferromagnetic nature. However, the indirect coupling between the spins of Mn ions and the conduction electrons is ferromagnetic (indirect superexchange) in nature [74]. In Ruderman–Kittel–Kasuya–Yoshida (RKKY) model, the interaction is based on the coupling between the magnetic ion and the conduction electron. However, if the electrons are localized, the RKKY interaction becomes weak and unrealistic. The mean-field Zener model proposed by Dietl et al. [19] is based on the original Zener model and the RKKY interaction and takes into account the anisotropy of the carrier mediated exchange interaction associated with the spin–orbit coupling in the host material. The Curie temperature (T_C) predicted by the mean-field Zener model in DMS material like (Ga, Mn) As is given by,

$$T_C = CN_{Mn}\beta^2 m^* p^{1/3} \quad (1.5)$$

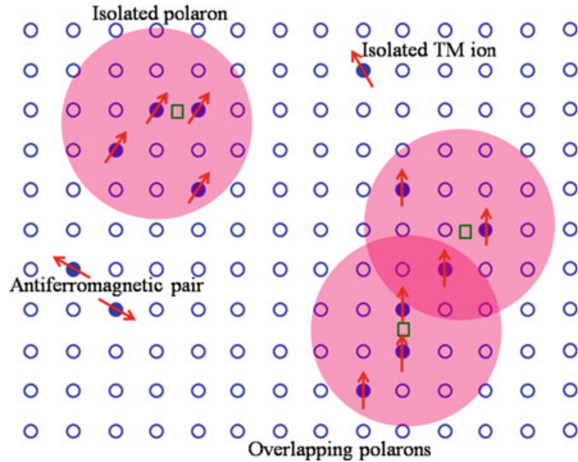

Fig. 1.8 Representation of magnetic polarons. A donor electron couples its spin antiparallel to impurities with a half-full or more than half-full 3*d* shell. Cation sites are represented by *small circles*. Oxygen is not shown; the unoccupied oxygen sites (F-center vacancies) are represented by *open squares*. Reproduced after permission from Nature Publishing group (*Nater. Mater*. 4, 175 (2005))

where N_{Mn} is the concentration of uncompensated Mn spins, β is the coupling constant (*p*–*d* coupling), m^* is the effective mass of the holes and *p* is the hole concentration.

First-principle ab initio calculations of electronic band structure by Sato and katayama-Yoshida [75] are based on the double exchange mechanism for the carrier-induced ferromagnetism. In the DMS material, if neighboring TM ions magnetic moments are in the same direction, the TM-*d* band is widened by the hybridization between the up–spin states. Therefore, in the ferromagnetic configuration the band energy can be lowered by introducing carriers in the *d* band. In these cases, the 3*d* electron in the partially occupied 3*d*-orbitals of the TM is allowed to hop into the 3*d*-orbitals of the neighboring TM, if neighboring TM ions have parallel magnetic moments. As a result, the *d*-electron lowers its kinetic energy by hopping in the ferromagnetic state. This is the so-called double exchange mechanism.

In addition to the above-mentioned models, the most recently proposed mechanism for the understanding of the ferromagnetic ordering of the TM ion due to the localized carriers is the BMP model [76]. The BMPs are formed by the alignment of the spins of many transition-metal ions with that of much lower number of weakly bound carriers such as excitons within a polaron radius. The basic idea is schematically illustrated in Fig. 1.8. The localized holes of the polarons act on the transition-metal impurities surrounding them, thus producing an effective magnetic field and aligning all spins. As temperature decreases, the interaction distance (boundary) grows. The neighboring magnetic polarons overlap and interact via magnetic impurities forming correlated clusters of polarons. One observes a ferromagnetic transition when the size of such clusters is equal to the size of the sample.

This model is inherently attractive for low-carrier density systems such as many of the electronic oxides. The polaron model is applicable to both *p*- and *n*-type host

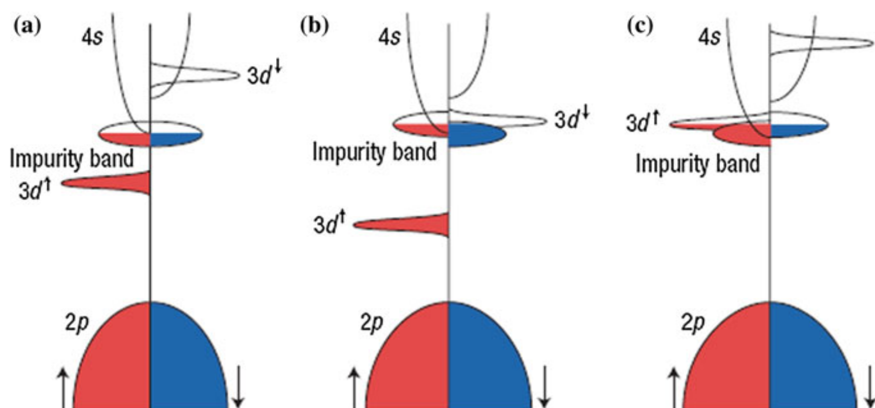

Fig. 1.9 Schematic band structure of an oxide with 3*d* impurities and a spin split donor impurity band. **a** The position of the 3*d* level for low Curie temperature T_C, when the splitting of the impurity band is small **b** and **c** show positions of the minority and majority spin 3*d* bands respectively that lead to high T_C. Reprinted after permission from Nature Publishing group (*Nater. Mater.* 4, 175 (2005))

materials. Even though the direct exchange interaction of the localized holes is antiferromagnetic, the interaction between BMPs may be ferromagnetic for sufficiently large concentrations of magnetic impurities. The ferromagnetic exchange is thus mediated by charge carriers in a spin–split impurity band formed by extending donor states. Coey et al. [76] have showed that for Sc, Ti, and V, the spinup states are aligned with the impurity levels and for Fe, Co, and Ni doping, the spindown states are aligned with the impurity levels. Mn and Cr dopings were said to have a small hybridization thereby leading to a weak magnetization. Figure 1.9 shows the schematic band structure of an oxide with 3*d* impurities and a spin–split donor impurity band.

1.3.3.2 Experimental Results of TM Ion Doped ZnO Thin Films and Bulk Polycrystalline Powders

Experimental attempts have led to various conflicting reports of room temperature ferromagnetism in ZnO [77, 78]. Both paramagnetism (Sharma et al. 2003) and ferromagnetism [79] have been observed in ZnO with TM^{2+} substituted at Zn^{2+}. Norton et al. [80] have showed the evidence of ferromagnetism with a Curie temperature around 250 K in Mn implanted *n*-type ZnO:Sn single crystal. High saturation magnetic moment of 1.4 μB/Mn is observed at room temperature in (Mn, N) codoped ZnO thin films grown by inductively coupled plasma enhanced chemical vapor deposition [81]. *Monte Carlo* simulation studies of Souza et al. [82] have showed that the *p*-type conductivity is essential for observing ferromagnetism in Mn-doped ZnO thin films. Hou et al. [83] have observed room temperature ferromagnetism in *n*-type Cu-doped ZnO thin films grown by DC